NUCLEAR ENGINEERING AND DESIGN 29 (1974) 110–124. © NORTH-HOLLAND PUBLISHING COMPANY

FINITE ELEMENT ANALYSIS OF LINEAR AND NONLINEAR HEAT TRANSFER*

E.L. WILSON, K.J. BATHE and F.E. PETERSON

Division of Structural Engineering and Structural Mechanics, Department of Civil Engineering, University of California, Berkelev, California 94720, USA

Received 10 September 1973

The finite element method is rapidly becoming a popular procedure for the evaluation of thermal stresses in complex structures. In linear analysis the method has been used extensively and has been coupled with stress analysis computer programs in order to automate thermal stress analysis. However, for the method to be effective, efficient numerical techniques need to be used. The purpose of this paper is to survey the recent developments in linear heat transfer analysis and, specifically, to present the techniques that permit the practical analysis of large and complex three-dimensional heat conduction problems. Typical practical problems are described and solution times are presented. In the analysis of systems with nonlinear thermal properties the method has had limited application. In this paper the general formulation of the incremental equations used in nonlinear heat transfer analysis are presented. An efficient numerical solution of the equations is given. Several types of nonlinearities are discussed and the solutions of some typical problems are presented.

1. Introduction

In recent years the finite element idealization has become a general approach for the stress analysis of complex structural systems. In order to minimize the preparation of data for a thermal stress problem it is desirable that the same finite element model is used in the stress and heat transfer analyses. For this reason considerable effort is currently being devoted to the development of compatible heat transfer and stress analysis programs.

For two-dimensional systems the method is well established and has been coupled with stress analysis computer programs in order to automate the transient thermal stress analysis procedure [1–3]. However, for three-dimensional systems and for systems with nonlinear thermal properties, the method has had limited applications [3–5].

In general the stress and heat transfer analyses of solids are coupled. In most cases, however, the significant structural effects are thermal stresses which do not affect the distribution of temperatures. Therefore, heat transfer analyses can be conducted separately before the stresses in the structures are determined. In such analyses nonlinearities may be due to temperature dependent material properties and, in particular, be caused by nonlinear boundary conditions.

To obtain economical solutions an efficient numerical implementation of the finite element analysis is important. Recent advances in the use of isoparametric elements have been found to be effective in the analysis of complex three-dimensional problems. The study of the stability and accuracy of the step-by-step integration procedure allows the selection of an effective time step increment.

The nonlinear heat transfer analysis of problems idealized by finite elements is currently in the developmental and experimental stage. In this paper procedures for the treatment of temperature dependent thermal properties and for nonlinear boundary conditions are given.

The purpose of this paper is to survey techniques that permit the practical analysis of complex three-dimensional linear heat conduction systems and the analysis of some nonlinear problems. The paper is

* Paper L1/4 presented at the Second International Conference on Structural Mechanics in Reactor Technology, Berlin, Germany, 10–14 September, 1973.

essentially a local view of the field, since it is largely based on the methods used at the University of California, Berkeley. Recent applications of the techniques in linear and nonlinear analyses are presented.

2. The finite element idealization

Many one, two, and three-dimensional field problems can be solved by subdividing the region into finite domains or elements. The field variables within each element are approximated by separate functions which have common values at the nodes of the element system. Such finite element solution exhibits various advantages when compared with other solution procedures. The mesh size can be varied and bodies of arbitrary shape can be considered without difficulty. Material properties can be different for each element and in general mixed boundary conditions can be handled directly. The equations which govern the response of the discrete system generally involve matrices which are symmetric and positive definite. Therefore, effective solution techniques can be employed for the solution of both the steady-state and transient problems.

In the initial application of the method, elements were restricted to the triangular and rectangular element families [1, 2, 6]. However, the development of the isoparametric family of elements has greatly extended the potential of the method. For this reason, it is worthwhile to summarize the implementation of isoparametric elements for heat transfer analysis.

A 4–8 node two-dimensional element is shown in fig. 1. The temperature within the element is expressed in the natural coordinate system x, y in terms of the temperatures at nodes 1–8,

$$\theta(x, y, t) = \sum H_i(x, y)\theta_i(t), \tag{1}$$

where

$$\begin{aligned}
H_1 &= \tfrac{1}{4}(1-x)(1-y) - \tfrac{1}{2}H_5 - \tfrac{1}{2}H_8,\\
H_2 &= \tfrac{1}{4}(1+x)(1-y) - \tfrac{1}{2}H_5 - \tfrac{1}{2}H_6,\\
H_3 &= \tfrac{1}{4}(1+x)(1+y) - \tfrac{1}{2}H_6 - \tfrac{1}{2}H_7,\\
H_4 &= \tfrac{1}{4}(1-x)(1+y) - \tfrac{1}{2}H_7 - \tfrac{1}{2}H_8,\\
H_5 &= \tfrac{1}{2}(1-x^2)(1-y),\\
H_6 &= \tfrac{1}{2}(1+x)(1-y^2),\\
H_7 &= \tfrac{1}{2}(1-x^2)(1+y),\\
H_8 &= \tfrac{1}{2}(1-x)(1-y^2),
\end{aligned} \tag{2}$$

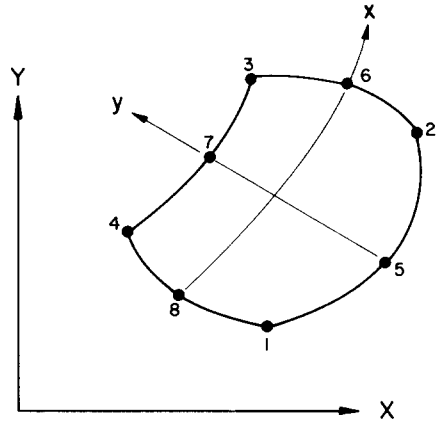

Fig. 1. 4–8 node two-dimensional isoparametric element.

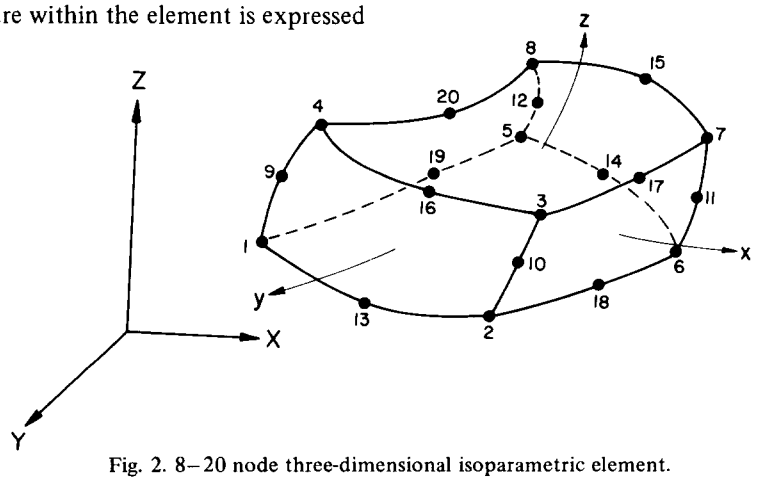

Fig. 2. 8–20 node three-dimensional isoparametric element.

One or all of nodes 5, 6, 7, and 8 can be omitted if the side is straight by setting the corresponding interpolation functions equal to zero. It is apparent that a single two-dimensional element with this flexibility is very useful in the idealization of complex geometries and for the variation of mesh size within a model.

An 8–20 node three-dimensional solid element is shown in fig. 2. The natural coordinates (x, y, and z) of the eight corner nodes are (± 1, ± 1, and ± 1) and of the 12 remaining nodes are $(0, \pm 1, \pm 1)$, $(\pm 1, 0, \pm 1)$, and $(\pm 1, \pm 1, 0)$. The temperature within the element is defined in terms of the nodal temperatures by

$$\theta(x, y, z, t) = \sum H_i(x, y, z)\theta_i(t). \tag{3}$$

To express the interpolation functions in a simple form it is convenient to define the following functions:

$$\begin{aligned} G(\beta, \beta_i) &= \tfrac{1}{2}(1 + \beta_i\beta), \quad \text{for } \beta_i = \pm 1 \\ &= 1 - \beta^2, \quad \text{for } \beta_i = 0 \end{aligned} \tag{4}$$

and

$$g_i = G(x, x_i)G(y, y_i)G(z, z_i), \tag{5}$$

where x_i, y_i, and z_i are the natural coordinates of the element nodal points. The interpolation functions are

$$\begin{aligned} H_1 &= g_1 - (g_9 + g_{13} + g_{19})/2, \\ H_2 &= g_2 - (g_{10} + g_{13} + g_{18})/2, \\ H_3 &= g_3 - (g_{10} + g_{16} + g_{17})/2, \\ H_4 &= g_4 - (g_9 + g_{16} + g_{20})/2, \\ H_5 &= g_5 - (g_{12} + g_{14} + g_{19})/2, \\ H_6 &= g_6 - (g_{11} + g_{14} + g_{18})/2, \\ H_7 &= g_7 - (g_{11} + g_{15} + g_{17})/2, \\ H_8 &= g_8 - (g_{12} + g_{15} + g_{20})/2, \\ H_j &= g_j \quad \text{for } j = 9, 10, 11, \ldots, 20. \end{aligned} \tag{6}$$

If any of the nodes 9–20 are omitted the corresponding value of g is zero.

Using the temperature interpolation functions, the element temperature is given by

$$\theta(x, y, z, t) = b(x, y, z)\theta(t), \tag{7}$$

and the element global derivatives of the temperature are

$$\theta(x, y, z, t)_{,i} = a(x, y, z)\theta(t). \tag{8}$$

In the evaluation of the isoparametric element matrices presented in the following section, it is necessary to use numerical integration. Hence, although the relations in eqs (7) and (8) are stated explicitly, in practice the matrices a and b are evaluated only at the integration points [2].

3. Equations for heat transfer analysis

The governing equations for the heat transfer analysis of a solid idealized by a system of finite elements may be derived by several different techniques. In the analysis of linear systems the minimization of a functional is a common approach [7, 8]. However, in nonlinear analysis a physical interpretation of the equations adds insight into the problem which may have certain advantages.

3.1. Physical statement of heat flow equilibrium

The heat transfer equations for a solid idealized by a system of finite elements can be physically interpreted as a statement of heat flow equilibrium at the nodes of the system at any time, i.e.

$$Q^{\mathrm{s}} + Q^{\mathrm{i}} = Q^{\mathrm{e}} + Q^{\mathrm{q}}, \tag{9}$$

where Q^{s} is the rate at which heat is stored within the elements adjacent to the node. In steady state conditions this term is zero at all nodes. Q^{i} is the rate of internal heat transfer by conduction in the elements adjacent to the node. Q^{e} is the rate at which heat enters the node from an external source. Q^{q} is the rate with which heat is generated within the elements adjacent to the node.

Using the physical properties of the finite elements the heat transfer rates can be expressed in terms of the temperatures at the element nodes.

The rate at which heat is stored within the material is

$$q^{\mathrm{s}} = c(\theta, t)\theta_{,t}, \tag{10}$$

where c is the material heat capacity and is, in general, a function of the temperature θ and the time t.

If the heat flow is defined as positive for a positive temperature gradient, the rate of heat transfer by conduction into direction j within the material is

$$q_j^i = \sum_n k_{jn}(\theta, t)\theta_{,n}, \tag{11}$$

where k_{jn} is the heat conductivity tensor of the material (which may also depend on θ and t), and n indicates the direction of temperature gradient. For orthotropic conductivity $k_{jn} = 0$ for $j \neq n$, and

$$q_j^i = k_{jj}(\theta, t)\theta_{,j}. \tag{12}$$

Using the material properties in eqs (10) and (11), the element interpolation functions in eqs (7) and (8) and invoking the virtual work principle to express the heat transfer rates in eq. (9) in terms of the nodal point temperatures [2], the matrix equation governing heat flow equilibrium is

$$C(\theta, t)\dot{\theta} + K(\theta, t)\theta = Q(t), \tag{13}$$

where C and K are the finite element system heat capacity and heat conductivity matrices respectively; and Q is the nodal point heat flow input.

3.2. System matrices

Denoting the direct stiffness procedure of assembling the system matrices from the element matrices by a summation sign, the matrices in eq. (13) are

$$C = \sum_{m=1}^{M} C_m; \qquad K = \sum_{m=1}^{M} K_m;$$

$$Q(t) = Q^e(t) + \sum_{m=1}^{M} Q_m(t), \tag{14}$$

where M is the total number of elements and $Q^e(t)$ is the vector of externally applied nodal heat flows.

The matrix C_m is the heat capacity matrix of element m,

$$C_m = \int_{V_m} b_m^T c_m b_m \, dV_m, \tag{15}$$

where c_m is the material heat capacity for the element.

In the studies carried out the heat capacity matrix could be approximated by a lumped diagonal matrix without a significant loss in accuracy [1, 9]. Such an approximation reduces computer storage and computational requirements by almost a factor of two.

The matrix K_m is the conductivity matrix of element m,

$$K_m = \int a_m^T k_m a_m \, dV_m, \tag{16}$$

in which k_m is the material conductivity tensor of the element.

The vector $Q_m(t)$ is the element thermal force vector

$$Q_m(t) = \int_{V_m} q_m(v, t) b_m^T \, dV_m + \int_{S_m} \bar{q}_m(s, t) b_m^T(s) \, dS_m, \tag{17}$$

in which $q_m(v, t)$ is the rate of heat generated within element m and $\bar{q}_m(s, t)$ is the rate of heat transfer at the boundary of surface element m.

4. Temperature boundary conditions

It should be noted that eq. (17) specifies boundary surface heat flow conditions and is used to prescribe insulated boundary surfaces by letting $\bar{q}(s, t)$ be equal to zero.

Another boundary condition which can be incorporated in a straightforward manner is the specification of nodal point temperatures. A commonly used procedure based on matrix partitioning was presented in ref. [1]. An alternative and often more effective approach to specify the temperature θ_i at node i is to modify the heat flow equilibrium equation, eq. (13), by adding a large conductivity value k_c to the ith diagonal element k_{ii} of K and specifying a heat flow input of $Q_i = k_c\theta_i$. Since $k_c \gg k_{ii}$, the calculated temperature at the node is θ_i. It should be noted that the distribution of the specified temperatures is restricted to the same form as the basic temperature field approximation within the elements adjacent to the node.

In the analysis of linear systems the elements of the conductivity and heat capacity matrices are constant, i.e. temperature and time independent. Sources of nonlinearities are, in general, temperature and time dependent conductivities and heat capacities and, in particular, more complex boundary conditions.

5. Numerical solution of heat flow equilibrium equations

5.1. Linear systems

Consider first the solution of eq. (13) in the analysis of linear systems. The temperature response of a system

can be calculated using the original finite element coordinate basis or using the basis of the thermal mode vectors [7, 14]. In the latter case the generalized eigenvalue problem to be considered is

$$K\phi = \lambda C\phi. \tag{18}$$

The solution of eq. (18) can be stated as

$$K\Phi = C\,\Phi\Lambda, \tag{19}$$

where Φ stores the C-orthonormalized eigenvectors (thermal mode vectors) $\phi_1, \ldots, \phi_n$ and Λ is a diagonal matrix listing the eigenvalues (thermal frequencies) $\lambda_1, \ldots, \lambda_n$. Using the transformation $\theta = \Phi X$, the heat flow equilibrium equations in the eigenvector basis are

$$\dot{X} + \Lambda X = \Phi^{\mathrm{T}} Q. \tag{20}$$

These equations are uncoupled and can readily be solved by a number of numerical procedures [10].

In practice, the transformation of the heat flow equilibrium equations to the eigenvector basis is, in most cases, not used because of the numerical operations required for the solution of eq. (18). Instead, the solution is obtained by direct integration of the heat flow equilibrium equations in the finite element coordinate basis [11]. However, it should be realized that the solution using the eigenvector basis would be more efficient if the primary heat flow response is contained in the first few thermal modes or if the response for a large number of time increments is required.

In the direct integration procedure currently employed, the solution to eq. (13) is obtained by assuming a linear variation of temperature over the time step Δt. This is a simple scheme which has proved to be efficient and accurate [9, 12]. It is of interest to note that an assumption of linear variation of the time rate of change of temperature results into a scheme which exhibits artificial oscillations in the solutions [1].

Using the assumption of linear temperature variation over the time step Δt we have at time τ

$$\dot{\theta}(\tau) = (1/\Delta t)(\theta_{t+\Delta t} - \theta_t) \tag{21}$$

and

$$\theta(\tau) = \theta_t + \{(\tau - t)/\Delta t\}(\theta_{t+\Delta t} - \theta_t), \tag{22}$$

where

$$t \leqslant \tau \leqslant t + \Delta t.$$

Hence, at time $t + \Delta t$,

Table 1.
Summary of step-by-step integration.

Initial calculation

(1) Form linear conductivity matrix K, heat capacity matrix C; initialize θ_0.
(2) Initialize the following constants tol. $\leqslant 0.01$; nitem $\geqslant 3$, $a_0 = 1/\Delta t$.
(3) Calculate $C^* = a_0 C$ and form effective conductivity matrix: $\boldsymbol{K} = K + C^*$.
(4) In linear analysis triangularize $\boldsymbol{K}$.

For each timestep

A. In linear analysis

(i) Compute effective heat flow vector: $\boldsymbol{Q}_t = Q_{t+\Delta t} + C^*\theta_t$.
(ii) Solve for nodal point temperatures at time $t + \Delta t$: $K\theta_{t+\Delta t} = \boldsymbol{Q}_t$.

B. In nonlinear analysis

(i) If a new conductivity matrix is to be formed, update for nonlinear conductivity effects to obtain $\boldsymbol{K}_t$; triangularize $\boldsymbol{K}_t$: $\boldsymbol{K}_t = LDL^{\mathrm{T}}$.
(ii) Form effective heat flow vector: $\boldsymbol{Q}_t = Q_{t+\Delta t} - F_t^{\mathrm{K}}$.
(iii) Solve for increments in nodal point temperatures using latest D, and L factors: $LDL^{\mathrm{T}}\Delta\theta_t = \boldsymbol{Q}_t$.
(iv) If required iterate for heat flow equilibrium; then initialize: $\Delta\theta_t^{(1)} = \Delta\theta_t$, $i = 0$.
  (a) $i = i + 1$.
  (b) Calculate ith approximation to nodal point temperatures and time derivatives of nodal point temperatures: $\theta_{t+\Delta t}^{(i)} = \theta_t + \Delta\theta_t^{(i)}$; $\dot{\theta}_{t+\Delta t}^{(i)} = a_0(\theta_{t+\Delta t}^{(i)} - \theta_t)$.
  (c) Calculate ith out-of-balance heat flow rates: $Q_{t+\Delta t}^{\mathrm{r}(i)} = Q_{t+\Delta t} - C\dot{\theta}_{t+\Delta t}^{(i)} - F_{t+\Delta t}^{\mathrm{K}(i)}$.
  (d) Solve for ith correction to temperature increments: $LDL^{\mathrm{T}}\Delta\Delta\theta_t^{(i)} = Q_{t+\Delta t}^{\mathrm{r}(i)}$.
  (e) Calculate new temperature increments: $\Delta\theta_t^{(i+1)} = \Delta\theta_t^{(i)} + \Delta\Delta\theta_t^{(i)}$.
  (f) Iteration convergence if $\|\Delta\Delta\theta^{(i)}\|_2 / \|\Delta\theta_t^{(i+1)} + \theta_t\|_2 <$ tol. If convergence: $\Delta\theta_t = \Delta\theta_t^{(i+1)}$ and go to (v). If no convergence and $i <$ nitem go to (a); otherwise restart using new conductivity matrix and/or a smaller time step size.
(v) Calculate new nodal point temperatures: $\theta_{t+\Delta t} = \theta_t + \Delta\theta_t$.

$$\dot{\theta}_{t+\Delta t} = (1/\Delta t)(\theta_{t+\Delta t} - \theta_t). \tag{23}$$

The solution for the temperature and its time variation at time $t + \Delta t$ is obtained by evaluating eq. (13) at time $t + \Delta t$ and substituting from eq. (23) for $\dot{\theta}_{t+\Delta t}$; the equation obtained is

$$\left(\frac{C}{\Delta t} + K\right)\theta_{t+\Delta t} = Q_{t+\Delta t} + \frac{C}{\Delta t}\theta_t. \tag{24}$$

Since the temperature at time t is known, eq. (24) yields

the temperature at time $t + \Delta t$. A computer program formulation of the step-by-step algorithm is given in table 1.

5.2. Stability analysis

To study the stability and accuracy of the integration scheme, it is noted first that the direct integration of the heat flow equilibrium equations in the original finite element coordinate basis, eq. (13), is equivalent to the direct integration of the uncoupled equations established in the thermal mode basis, eq. (20). Hence for the purpose of a stability analysis we need only study the integration algorithm as applied to a typical equation i in eq. (20), which can be written as

$$\dot{x} + \lambda_i x = q, \tag{25}$$

where $q = \phi_i^T Q$. We now have

$$\dot{x}_{t+\Delta t} = (1/\Delta t)(x_{t+\Delta t} - x_t) \tag{26}$$

and want to solve

$$\dot{x}_{t+\Delta t} + \lambda_i x_{t+\Delta t} = q_{t+\Delta t}. \tag{27}$$

Substitution of $\dot{x}_{t+\Delta t}$ from eq. (26) into eq. (27) yields

$$x_{t+\Delta t} = A x_t + L q_{t+\Delta t} \tag{28}$$

in which

$$A = \frac{1}{1 + \lambda_i \Delta t}, \quad \text{and} \quad L = \frac{\Delta t}{1 + \lambda_i \Delta t}. \tag{29}$$

The quantity A is the difference approximation operator and L is the heat flow operator as applied to the ith uncoupled nodal heat flow equation.

The recursion relation in eq. (28) can be used to study the stability and accuracy of the integration scheme [11]. Note that the solution at time $t + m\Delta t$ is

$$x_{t+m\Delta t} = A^m x_t + A^{m-1} L q_{t+\Delta t} + \ldots + L q_{t+m\Delta t}. \tag{30}$$

The integration method is unconditionally stable if $A^m m \to \infty$ is bounded for any time step Δt. This means that the stability condition is

$$A \leqslant 1. \tag{31}$$

From eq. (29) we need

$$1 + \lambda_i \Delta t \geqslant 1.$$

Since the thermal frequency $\lambda_i \geqslant 0$ the integration algorithm is unconditionally stable. The accuracy of the integration clearly depends on $\lambda_i \Delta t$ and can conveniently be studied using eq. (30).

5.3. Nonlinear systems

In the analysis of nonlinear systems direct integration must be used. Assuming that only temperature dependent conductivity effects are present, eq. (13) at time $t + \Delta t$ is

$$C\dot{\theta}_{t+\Delta t} + K_{t+\Delta t}\theta_{t+\Delta t} = Q_{t+\Delta t}, \tag{32}$$

where $K_{t+\Delta t}$ is the system conductivity matrix at time $t + \Delta t$. For a solution we use the approximation

$$K_{t+\Delta t}\theta_{t+\Delta t} = F_t^K + K_t \Delta\theta_t, \tag{33}$$

where F_t^K is the internal heat flow due to conduction at time t evaluated directly using the thermal conductivities at the temperature θ_t, K_t is the system conductivity matrix at time t, and

$$\Delta\theta_t = \theta_{t+\Delta t} - \theta_t. \tag{34}$$

Using eqs (23) and (32)–(34) an equation is obtained for the temperature increment $\Delta\theta_t$, i.e.

$$\{(C/\Delta t) + K_t\}\,\Delta\theta_t = Q_{t+\Delta t} - F_t^K. \tag{35}$$

In many cases this simple incremental solution procedure yields accurate solutions and is equivalent to applying eq. (24) in which K is updated in each time step. However, the errors introduced by the linearization in eq. (33) may be corrected by iteration for heat flow equilibrium. Table 1 gives an efficient computer program formulation of the incremental solution procedure with the option of heat flow equilibrium iteration.

In table 1 only temperature dependent thermal conductivities are considered; however, the step-by-step solution for heat flow equilibrium in each time step is quite general and is similar when different classes of nonlinear boundary conditions, some of which are presented in the next section, or time dependent thermal properties are included.

6. Additional boundary conditions

The specification of nodal point temperatures and sur-

face heat flows has already been discussed. Some additional important boundary conditions are presented in the following.

6.1. Convection boundary condition

In the case of free convection the rate of heat transfer $q(x, y, t)$ across a boundary layer is given by

$$q(x, y, t) = h\{\theta_e(t) - \theta(t)\}^{\alpha}, \tag{36}$$

where h is the convection coefficient, $\theta_e(t)$ is the temperature of the external environment, and $\theta(t)$ is the temperature of the surface of the solid. In an incremental solution the surface temperature is known at time t and unknown at time $t + \Delta t$. Therefore, an approximate heat flow at time $t + \Delta t$ can be evaluated if the surface temperature at time t is used. Note that depending on the nonlinearities introduced by h and α and the solution accuracy required, it may be necessary to use a heat flow equilibrium iteration.

For $\alpha = 1$ and h not a function of temperature, the boundary condition is linear and can be specified exactly. In this case, eq. (36) yields concentrated nodal heat flows

$$Q_i(t) = h \int H_i(x, y)\theta_e(t)\, dA - h \int H_i(x, y)\theta(t)\, dA. \tag{37}$$

Assuming that the temperatures vary as

$$\theta_e(t) = \sum H_j(x, y)\theta_{ej}(t); \qquad \theta(t) = \sum H_j(x, y)\theta_j(t), \tag{38}$$

where the summation is taken over the appropriate interpolation functions, the nodal heat flows are given by

$$Q_i(t) = Q_i(t)^* - \sum k_{ij}^* \theta_j(t) \tag{39}$$

in which

$$k_{ij}^* = \int hH_i(x, y)H_j(x, y)\, dA, \quad Q_i^*(t) = \sum k_{ij}^* \theta_{ej}(t). \tag{40}$$

In the solution, therefore, the terms k_{ij}^* of eq. (40) need be added to the appropriate elements of the heat conductivity matrix, and the terms $Q_i^*(t)$ contribute to the externally applied system heat flow vector.

Considering nonlinear boundary conditions, if h is constant but $\alpha > 1$, it may be an effective approach to incorporate the boundary condition to separate the heat flow in eq. (36) approximately into linear and nonlinear contributions,

$$q = h\{\rho_e(t) - \theta(t)\} + f\{\theta_e(t), \theta(t), \alpha\}. \tag{41}$$

The linear contribution can be accounted for exactly, and the nonlinear contribution can be evaluated approximately, as described above.

6.2. Radiation boundary condition

The Stefan–Boltzmann relation for the heat radiation of a surface is [13]

$$q = \kappa\{\bar{\theta}_e^4(t) - \bar{\theta}^4(t)\}\, dA, \tag{42}$$

where $\bar{\theta}_e(t)$ and $\bar{\theta}(t)$ are absolute temperatures of the environment and the surface, respectively, and κ is a constant. Writing eq. (42) in the form

$$q = [\kappa\{\bar{\theta}_e^2(t) + \bar{\theta}^2(t)\}\{\bar{\theta}_e(t) + \bar{\theta}(t)\}]\{\theta_e(t) - \theta(t)\}, \tag{43}$$

the boundary condition is recognized to be of the form of the convection boundary condition with $\alpha = 1$ and

$$h = \kappa\{\bar{\theta}_e^2(t) + \bar{\theta}^2(t)\}\{\bar{\theta}_e(t) + \bar{\theta}(t)\}.$$

6.3. Surface cooled by moving fluid

The boundary condition imposed by a fluid or gas moving along the surface of a body is of the same general form as the convection boundary condition. The cooling of the surface is effected by a rate of heat transfer $q(x, y, t)$ across a boundary layer given by

$$q = h\{\theta_e(t) - \theta(t)\}\, dA, \tag{44}$$

where h may be a function of θ, θ_e, and v; θ is the temperature of the surface, θ_e is the temperature of the moving fluid, and v is the velocity of the fluid. If the fluid is confined, the temperature of the fluid will be known only at the source and may change signifi-

cantly along the surface of the body due to heat transfer effects between the liquid and the solid. Therefore, eq. (44) cannot be applied directly. A solution can be obtained if it is assumed that the heat conduction within the fluid is negligible when compared with the heat transferred by the mass transfer of the moving fluid. Consider the surface shown in fig. 3. The temperature of the fluid at point a is known. The temperatures within the fluid must satisfy heat flow equilibrium; therefore the following equation must be satisfied for the rate of heat flow at nodes i and j of the pipe:

$$Q_j = Q_i - Q_{ij}, \tag{45}$$

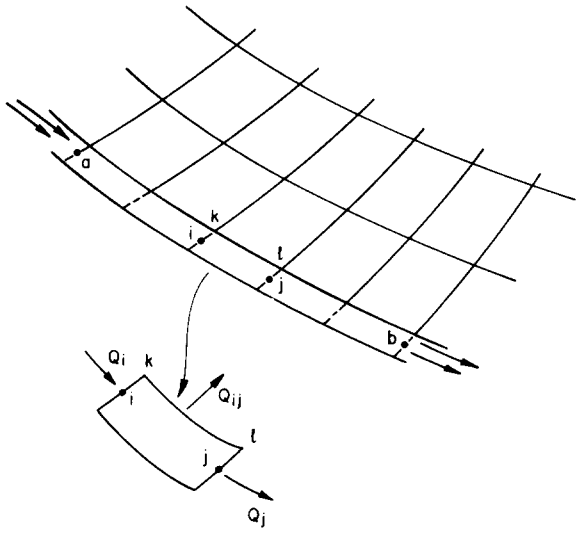

Fig. 3. Surface subjected to moving fluid.

where

$$Q_j = \rho v c \theta_j, \qquad Q_i = \rho v c \theta_i, \tag{46}$$

ρ is the fluid density, c is the specific heat of the fluid, and v is the fluid flow rate. Assuming that

$$Q_{ij} = A_{kl} h_{kl} \{\theta_e(t) - \theta(t)\}; \qquad \theta_e(t) = \frac{\theta_i + \theta_j}{2};$$

$$\theta(t) = \frac{\theta_k + \theta_l}{2}, \tag{47}$$

where A_{kl} is the surface area between nodes k and l and h_{kl} is the heat transfer coefficient for the surface considered, eq. (45) can be expressed in terms of the temperatures θ_i, θ_j, θ_k, and θ_l. Thus the following recursive relationship is obtained to compute the temperature of the moving fluid from point a to point b:

$$\theta_j = \{(1 - \gamma)\theta_i + \gamma\theta_k + \gamma\theta_l\}/(1 + \gamma), \tag{48}$$

where

$$\gamma = A_{kl} h_{kl} / 2\rho c v.$$

Equation (48) is used in each time step to compute the temperature $\theta_e(t)$ of the moving fluid. The boundary condition of the surface cooled by the moving fluid can then be approximately incorporated in the same way as the convection boundary condition was enforced.

Table 2.
Problem statistics for linear solutions (calculated with program TAP [12]).

Model	Number of time steps	Isoparametric elements		Number of equations	Half bandwidth	Solution times*
		four-node	eight-node			
(1) Horsecollar pumping house	steady state	160	467	1129	198	152 CP 124 IO
(2) Structure	steady state	0	2000	2873	309	339 CP 266 IO
(3) Pump housing	steady state	360	146	994	234	102 CP 105 IO
	37	360	146	994	234	175 CP 330 IO

* Computations performed on the CDC 6600 computer, Data Services Division SCOPE 3.3; CP are central processor seconds, and IO are secondary storage peripheral processor seconds.

7. Sample solutions

A large number of practical analyses of linear systems have been performed using the computer program TAP, which employs the numerical techniques discussed in this paper [12]. Table 2 gives some typical solution times.

The analyses described in the following have been part of various practical investigations of linear and nonlinear heat transfer in solids and structural components.

7.1. Linear transient heat conduction analysis of a semi-infinite solid subjected to a unit heat flux

A semi-infinite solid initially at zero temperature is exposed to a constant heat flux of unit intensity at

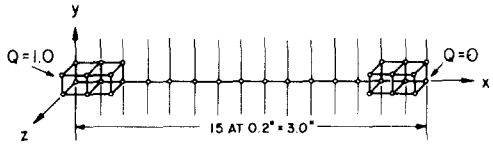

Fig. 4. 15 element model of a semi-infinite solid.

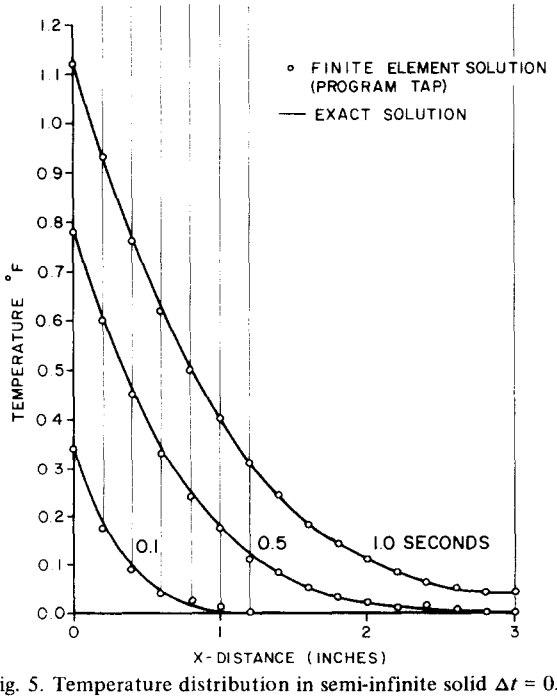

Fig. 5. Temperature distribution in semi-infinite solid $\Delta t = 0.05$ sec.

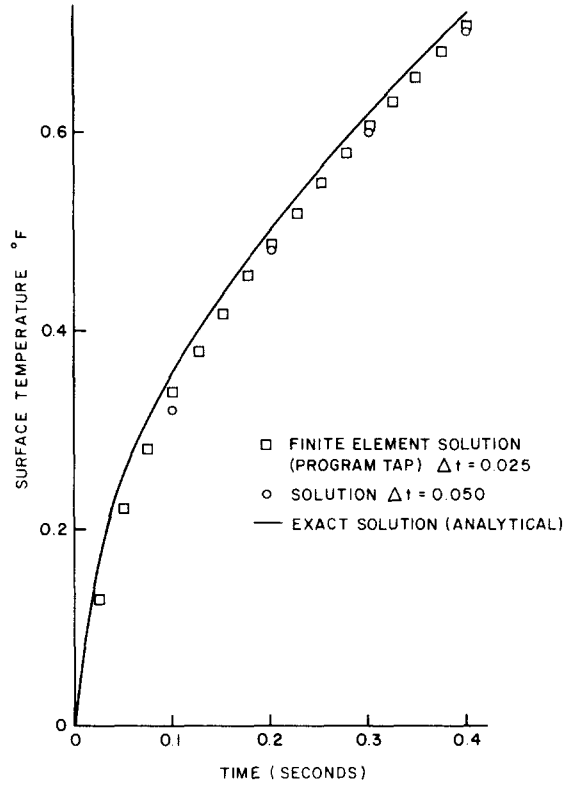

Fig. 6. Surface temperature of semi-infinite solid versus time from start of heating.

time $t = 0+$; i.e. $Q(0, t) = 1.0$, $t > 0$. Linear, i.e. time and temperature independent, material properties are assigned unit values; i.e. $k = 1.0$, $\rho = 1.0$, and $c = 1.0$.

In the analysis 15 equal length eight node solid elements are used to represent a 3 in. depth of the semi-infinite solid, fig. 4. The surface of the solid coincides with the y, z plane. The four nodes on the interior $x = 3$ in. plane are assumed to be insulated, and the nodes on the $x = 0$ element face are subjected to the unit value of heat flux. Two solutions were run using the same model, but with different time steps; namely $\Delta t = 0.025$ and 0.050 sec.

If x represents the distance into the solid, then the temperature distribution is given by [13]

$$\theta(x, t) = 2\{(t/\pi)^{1/2} \exp(-x^2/4t) - (x/2) \times \operatorname{erf} c(x/2\sqrt{t})\}.$$

Figure 5 shows the temperature distributions into the depth of the solid at time 0.1, 0.5, and 1.0 sec. A plot of the solid's surface temperature versus time is given in fig. 6. It is noted that the finite element solu-

tion accurately predicts the temperature response of the solid.

7.2. Nonlinear steady-state heat conduction in an infinite, parallel sided slab

A slab of thickness Δx and infinite in extent is exposed on the one face at $x = 0$ to the linear convection boundary condition $q = h(\theta_e - \theta_1)$, in which the environmental temperature θ_e is taken to be time independent, and θ_1 is the unknown temperature of the face. The other face at $x = \Delta x$ is maintained at the constant temperature θ_2, fig. 7. The thermal conductivity of the slab material is taken to be a linear function of temperature, i.e. $k = b + m\theta$.

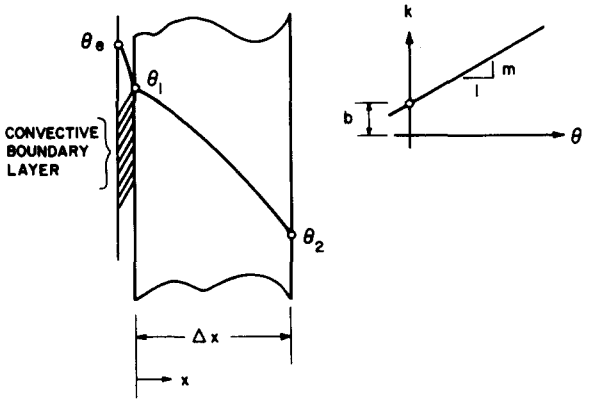

Fig. 7. Steady-state nonlinear heat conduction through a slab.

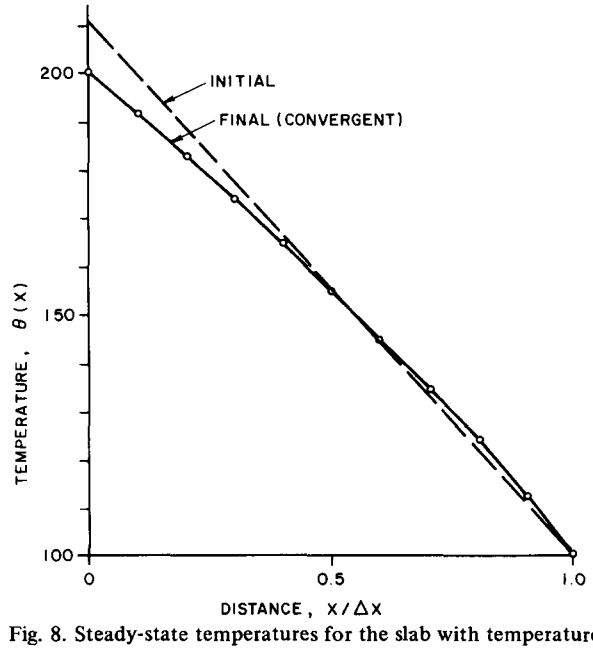

Fig. 8. Steady-state temperatures for the slab with temperature dependent conductivity.

The solution for θ can be obtained analytically using the condition of thermal equilibrium at the face $x = 0$. This condition requires that $\theta_1^2 + B\theta_1 + c = 0$, where

$$B = (2b/m + 2\Delta x h/m),$$

$$C = -(2b\theta_2/m + 2\Delta x h\theta_e/m + \theta_2^2).$$

Choosing the following values for the parameters: $\Delta x = 0.5$, $m = 2$, $b = 200$, $h = 1000$, $\theta_e = 300$, and $\theta_2 = 100$, the solution for θ_1 is 200.

In the finite element analysis for the temperature distribution ten equal length one-dimensional elements were used to represent a unit cross section through the slab thickness Δx. The solution is obtained using the iteration for heat flow equilibrium given in table 1. Since a steady-state analysis is performed the heat capacity of the system is neglected, and the analysis is only performed for one time step. Fig. 8 shows the predicted distribution of temperatures through the thickness of the slab. The broken line is the temperature profile predicted with zero initial estimates of node temperatures, i.e. for $\theta = 0$ at all nodes initially, $k = b$ for all elements. The solid curve plots predicted temperature values resulting from four cycles of iteration after which successive iterations predict the same temperatures to five digits (i.e. tol. = 0.0001 in table 1).

7.3. Transient temperature analysis of a mass concrete structure during construction

The purpose of this problem is to predict temperature distributions in a mass concrete structure due to heat generation produced by the curing concrete. The resulting temperature distributions are then used to predict thermal stresses in the concrete at various points in time from start of construction [9].

The structure is the concrete containment for four penstocks (11 m in diameter) running under an earth-fill dam. One half of a typical transverse section of the structure is shown schematically in fig. 9. Note that the concrete is placed in two base lifts (l_1 and l_2); then, the steel liners for the penstocks are installed and finally the envelopment lifts (L1–L9) are placed. The

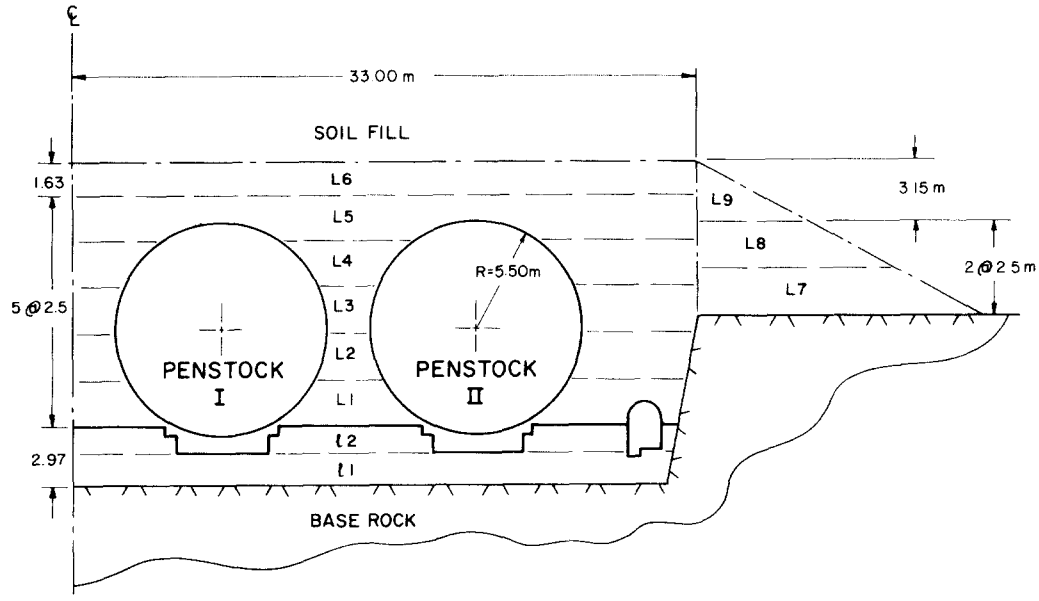

Fig. 9. Transverse section of the penstock structure showing concrete placement sequence.

finite element representation of the penstock section is shown in fig. 10. The model includes a portion of the base rock, and element boundaries in the concrete mass coincide with actual lift placement boundaries.

In order to account for the effects of the actual construction sequence, the element material properties and the rates of internal heat generation in the concrete must be time dependent, i.e. before the concrete is in place c_m (eq. (15)), k_m (eq. (16)) and $q(v, t)_m$ (eq. (17)) are all zero. After the concrete has been placed c_m and k_m for all existing elements are assumed constant, and the rate of internal heat generation for the newly placed elements is as shown in fig. 11.

Boundary conditions assumed in the analysis are listed as follows:

(1) existing concrete surfaces are exposed to linear, free convection, i.e. eq. (36) with constant h and $\alpha = 1$; the environmental temperature θ_e is constant for any one month, but varies from month to month (20°C in June to 27°C in December);

(2) the base rock boundary is insulated; and

(3) the inside surface of the penstocks are cooled to a constant 17°C.

Figure 12 is a plot of isothermal contours in the concrete section 100 days from the start of construction; note that construction is complete only through lift L5. A similar set of contours is plotted in fig. 13 showing the temperature distribution in the completed structure at 140 days.

The thermal stresses induced by cooling from maximum temperatures were found to be significant in the top lift (L6); as a result some horizontal reinforcement was included to prevent cracking in the uppermost section of the structure.

7.4. Nonlinear transient temperature analysis of an infinite parallel sided slab

Consider the slab of thickness 20 and infinite in extent shown in fig. 14. The slab is kept at a reference temperature 100. At time 0+ the temperature at its left face is raised to 200 until at time 10 the temperature drops back to 100, fig. 14. The thermal conductivity k is assumed to vary as a function of temperature as given in fig. 14; the heat capacity c is constant and equal to 8. This problem was analyzed in ref. [4]. In the analysis the slab is represented by 20 equally spaced one-dimensional elements to represent a unit cross section through the slab thickness. The transient temperature distributions are obtained using the algorithm with heat flow equilibrium iteration in table 1, where $\Delta t = 1$ and tol. = 0.00001 are selected. Three analyses are performed in which, respectively, new conductivity matrices are formed and triangularized (1) in each time

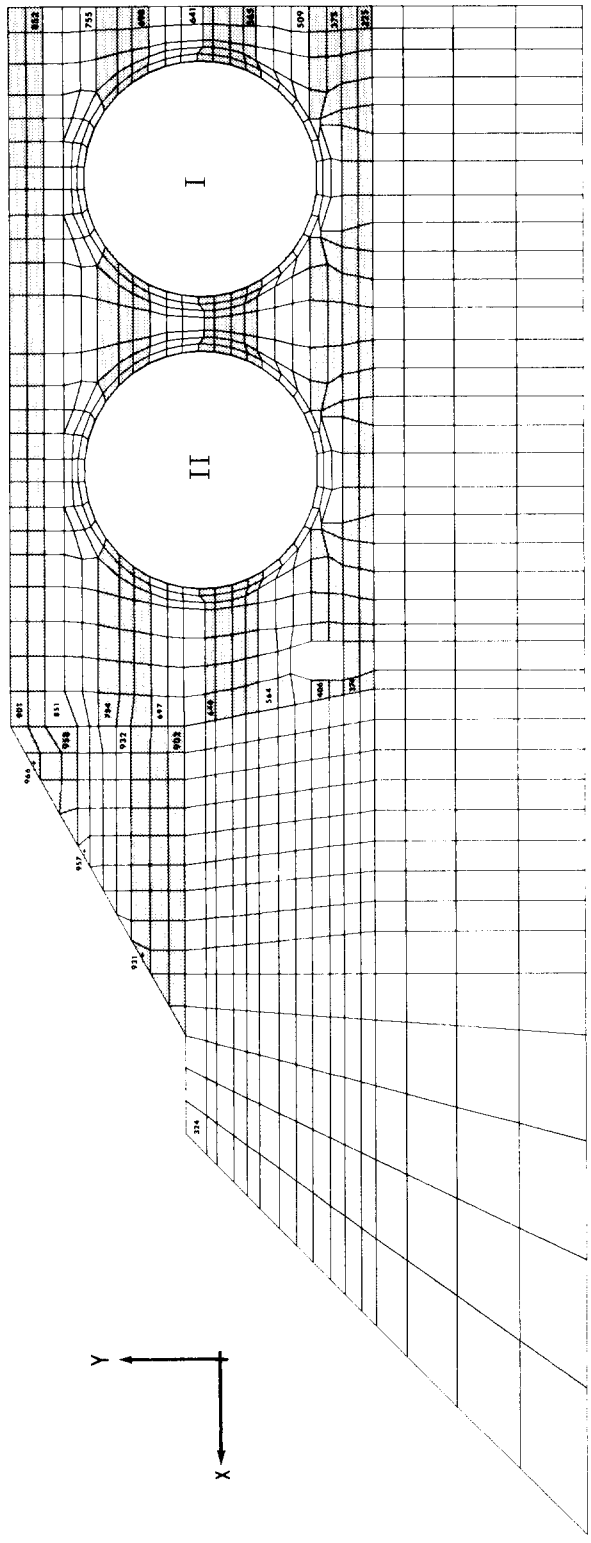

Fig. 10. 966 element representation of one symmetric half of the Capivara penstocks.

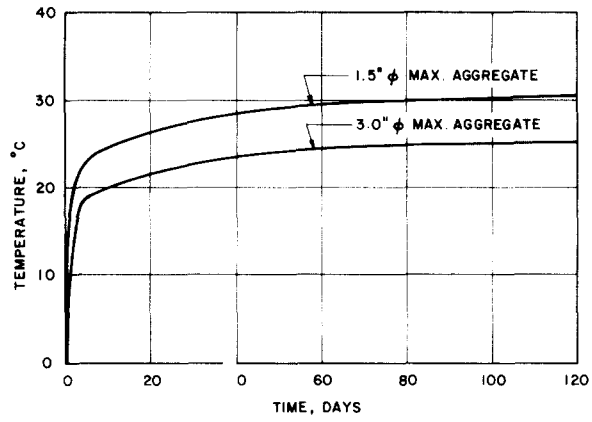

Fig. 11. Adiabatic temperature rise for the concrete.

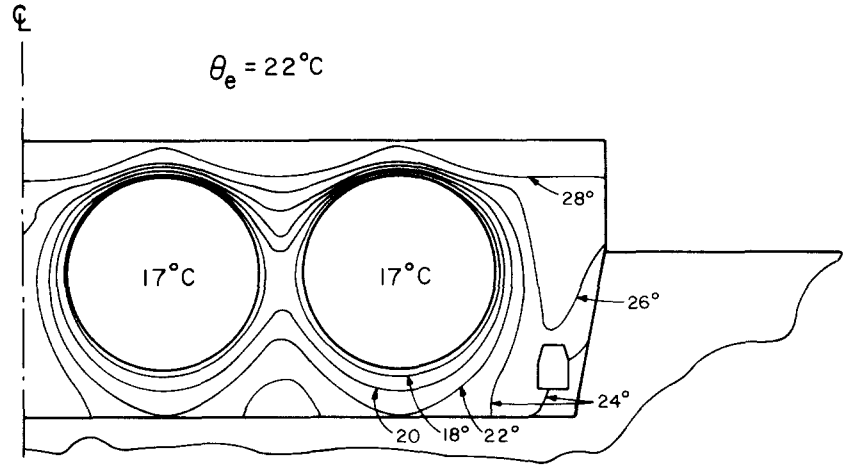

Fig. 12. Temperature contours in concrete 100 days from start of construction.

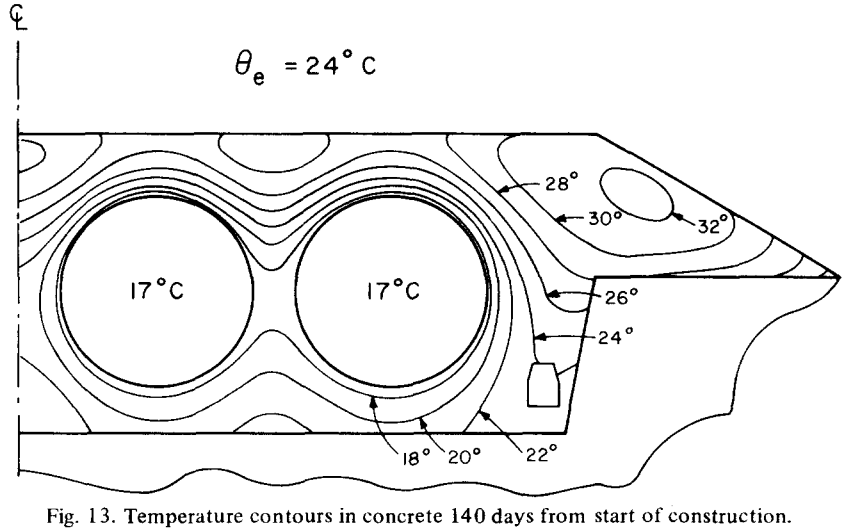

Fig. 13. Temperature contours in concrete 140 days from start of construction.

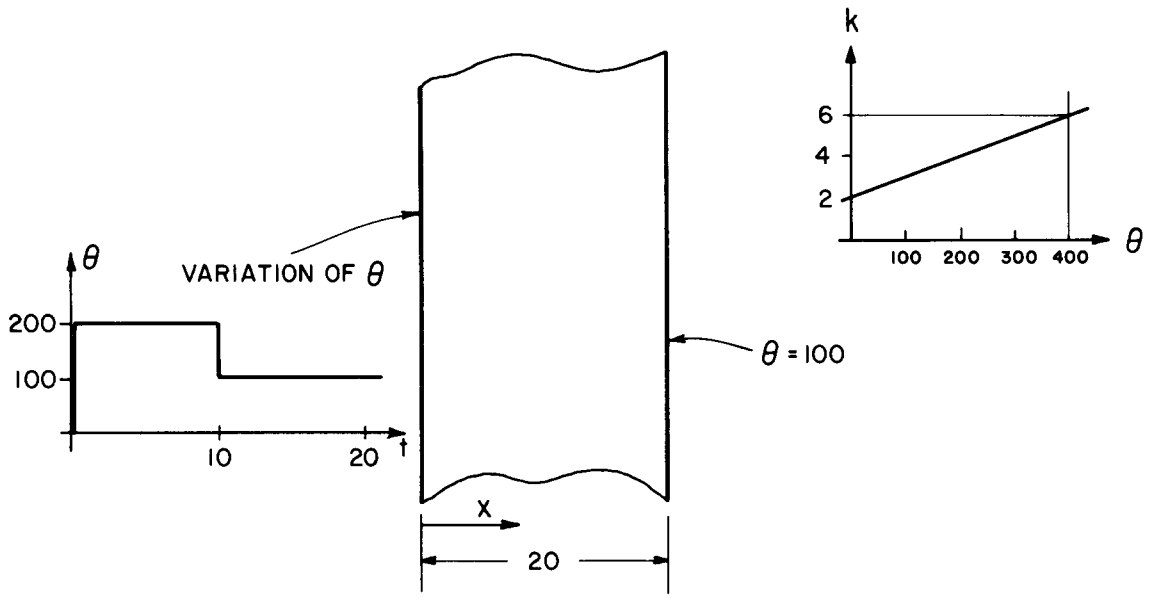

Fig. 14. Nonlinear transient heat conduction through a slab.

step, (2) in every fifth time step, and (3) only once at the start of solution when $\theta = 100$. The temperature distributions calculated in the three analyses are the same to about five digits, and the average number of iterations in the analyses are 2, 3, and 5, respectively. Table 3 gives the temperature at distance x from the left face of the slab at times $t = 10$ and 11. In ref. [4] the solution is given in a small figure, but to the accuracy possible to be observed, the results given in table 3 are in good agreement.

Table 3.
Temperatures at distance x from the left face of the slab, $t = 10$ and $t = 11$.

Distance x	θ at $t = 10$	θ at $t = 11$
0	200.00	100.00
1	187.35	141.52
2	174.68	153.46
3	162.38	153.19
4	150.83	147.68
5	140.38	140.23
6	131.26	132.52
7	123.59	125.41

8. Conclusions

Finite element analysis techniques for linear and nonlinear heat transfer have been presented. The general formulations of the relevant equations of heat flow equilibrium and boundary conditions have been discussed and an effective step-by-step solution procedure has been given. Sample analyses have been presented to show some applications of the solution techniques.

References

[1] E.L. Wilson and R.E. Nickell, Application of the finite element method to heat conduction analysis, Nucl. Eng. Des. 4 (1966) 276–286.
[2] O.C. Zienkiewicz, The Finite Element Method in Engineering Science, McGraw-Hill (1971).
[3] W.A. Shuker, A survey of heat-conduction computer programs, Nucl. Safety 12 (1971) 569–582.
[4] G. Aguirre-Ramirez and J.T. Oden, Finite-element technique applied to heat conduction in solids with temperature dependent thermal conductivity, ASME, Winter Annual Meeting, Los Angeles, California, Nov. 1969.
[5] P.D. Richardson and Y.M. Shum, Use of the finite element methods in solution of transient heat conduction problems, ASME, Winter Annual Meeting, Los Angeles, California, Nov. 1969.
[6] W. Visser, A finite element method for the determination of non-stationary temperature distribution and thermal

deformations, Proc. Conf. on Matrix Methods in Structural Mechanics, Air Force Institute of Technology, Wright Patterson AFB, Ohio (1965).

[7] M.A. Biot, New methods in heat flux analysis with application to flight structures, J. Aeronaut. Sci. 24 (1957) 857–873.

[8] M.E. Gurtin, Variational principles for linear initial-value problems, Quart. Appl. Math. 22 (1964) 252–256.

[9] E.L. Wilson, The determination of temperatures within mass concrete structures, SESM Report, 68–17, University of California, Berkeley (1968).

[10] L. Collatz, The Numerical Treatment of Differential Equations, 3rd edn, Springer, New York (1966).

[11] K.J. Bathe and E.L. Wilson, Stability and accuracy analysis of direct integration methods, Int. J. Earthquake Eng. Struct. Dyn. 1 (1973) 283–291.

[12] F.E. Peterson and H. Hiu, Three-dimensional heat transfer analyses using a finite element procedure – theoretical basis and sample solutions, Engineering/Analysis Corporation, Report, 4.1.4.1, Aug. (1971).

[13] H.S. Carslaw and J.C. Jaeger, Conduction of Heat in Solids, 2nd edn, Clarendon Press (1959).

[14] R.H. Gallagher and R. Mallet, Efficient solution processes for finite element analysis of transient heat conduction, ASME, Winter Annual Meeting, Los Angeles, California, Nov. 1969.